



Wi-Limb: Recognizing Moving Body Limbs Using a Single WiFi Link

Soumita Ghosh
ghoshs9@vcu.edu

Department of Computer Science
Virginia Commonwealth University
Richmond, Virginia, USA

Eyuphan Bulut
ebulut@vcu.edu

Department of Computer Science
Virginia Commonwealth University
Richmond, Virginia, USA

ABSTRACT

Utilizing fine grained analysis of wireless signals for human activity recognition has gained a lot of traction recently. The unique changes to the ambient wireless signals caused by different activities made it possible to recognize these fingerprints through deep learning classification methods. Most of the existing work consider a set of physical activities or gestures and try to recognize each one of them as a separate class. However, this makes the classification task harder especially when the number of activities to recognize becomes larger and when these activities include movements from the same body parts. To address that, in this study, we consider the decomposition of each physical activity into the limbs and body parts involved in that activity and study a one-by-one recognition solution. We propose a Generative Adversarial Network (GAN)-based hierarchical method that not only recognizes the involved body limbs and facilitates the recognition of complex activities, but also mitigates the temporal effects in the collected signal data and thus provides a generalized solution. Our experimental evaluation shows that we can recognize unknown physical activities through the proposed hierarchical limb recognition based model with a small Hamming loss and by just using WiFi signal data from a single transmitter and receiver link.

CCS CONCEPTS

• **Human-centered computing** → Ubiquitous and mobile computing systems and tools; • **Hardware** → Wireless integrated network sensors; • **Computing methodologies** → Machine learning.

KEYWORDS

WiFi sensing, physical activity monitoring, Channel State Information.

ACM Reference Format:

Soumita Ghosh and Eyuphan Bulut. 2024. Wi-Limb: Recognizing Moving Body Limbs Using a Single WiFi Link. In *The 30th Annual International Conference on Mobile Computing and Networking (ACM MobiCom '24)*, November 18–22, 2024, Washington D.C., DC, USA. ACM, New York, NY, USA, 7 pages. <https://doi.org/10.1145/3636534.3698117>



This work is licensed under a Creative Commons Attribution International 4.0 License. *ACM MobiCom '24, November 18–22, 2024, Washington D.C., DC, USA*
© 2024 Copyright held by the owner/author(s).
ACM ISBN 979-8-4007-0489-5/24/11.
<https://doi.org/10.1145/3636534.3698117>

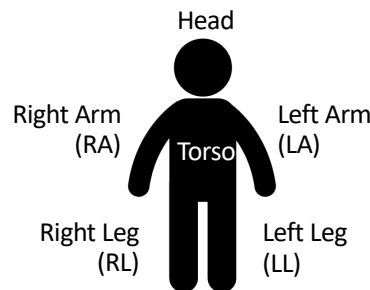


Figure 1: Main body limbs involved in a physical activity.

1 INTRODUCTION

Monitoring physical activities of people is an essential tool for rehabilitation, healthy aging and well-being of individuals [1]. It can also help early diagnosis of several medical issues and disorders and can result in more effective treatment and recovery [16, 28].

Thanks to the recent advances in mobile and wearable device technology, one can now easily track their physical activities and additional health related metrics like heart rate and blood pressure with a wearable device attached to their body (e.g., Fitbit, smart watch). The ubiquitous availability of such devices also motivates people to perform more physical activities for a healthy lifestyle [15] as they can use the feedback from these devices to balance their diet and exercise accordingly.

While the usage of such wearables is pretty common today, the studies show that there are a lot of variations in the measurements done with different types of devices and they can work in certain scenarios or for people with certain physical features. These devices will also be limited to measuring the movement of the body part they are attached to. Thus, in order to track different limb movements, a separate sensor or wearable attached to each of these limbs [27] would be required, making it a cumbersome solution. Moreover, these devices require periodic maintenance, such as recharging or replacing batteries and may not be comfortable to wear for some people all the time. That is why the usage of wearables is less common among old adults compared to young adults [35]. While the adoption rate among old adults is growing, further studies are needed to motivate the usage of mobile health tracking devices by older adults [23].

Alternatively, in this study, we consider a wireless sensing based non-invasive, minimal or no maintenance requiring, and low-cost solution to track the moving body parts during physical activities. In particular, we consider the utilization of ambient WiFi signals and

the associated Channel State Information (CSI) over all subcarriers for this purpose. Most of the existing WiFi sensing solutions [3, 9, 10, 30] consider recognition of a set of activities (e.g., sitting, walking, drinking) using the CSI data collected from WiFi signals. Different from these studies, in this study, we specifically explore the recognition of moving body limbs through WiFi sensing. To this end, we consider five different main body parts attached to human torso as shown in Fig. 1 and decompose each physical activity into the movement of these body parts. Then, we explore a hierarchical approach that aims to recognize the limbs involved in a physical activity one by one. To achieve this goal, our approach not only identifies the next limb involved in the physical activity based on the currently recognized ones, but also determines when to stop including new limbs.

Multi-limb activity recognition can be helpful in various ways. It can help monitoring patients with movement disorders or those recovering from any limb surgery (e.g., rehabilitation exercises). It can also contribute to detecting multi-limb movements during sleep. For instance, Periodic Limb Movement Disorder (PLMD) occurs when a patient moves one or more limbs frequently and periodically during sleep [13, 31]. Detecting this disease is challenging, especially for elderly individuals living alone. Moreover, by knowing which body limbs are moving (and potentially how fast they are moving), it may be possible to estimate the energy expenditure or calories burned associated with a physical activity without any wearables [34]. Thus, our proposed solution can be a valuable tool for all these purposes.

The rest of the paper is organized as follows. We first review related work on limb movement recognition methods and WiFi sensing in Section 2 and highlight the differences of this study. In Section 3, we then elaborate on the proposed method. Next, we provide the evaluation of the proposed solution together with how the data is collected and processed in Section 4. Finally, we provide our concluding remarks and discuss on future work in Section 5.

2 RELATED WORK

Identification and tracking of moving limbs has been studied extensively using computer vision techniques. With the advances in deep learning algorithms and increasing number of available datasets with human pose information, this type of research has also been growing [2, 19, 20]. However, such computer vision-based solutions require a line-of-sight visibility of the human and thus are limited to certain scenarios. It is also affected by lighting conditions or any obstructions in the environment. On top of these, they also come with privacy related concerns by the users and they have high deployment costs due to the cameras or other related equipment involved.

Wearable sensor based approaches [17, 24, 25] mitigate some of these problems (e.g., cost, privacy) by installing several types of wearable sensors on the human body and utilizing statistical and learning based solutions on the collected data. These sensors include IMU sensors, accelerometers and smartwatches. While it has been shown that some sufficient accuracy can be achieved in the identification of moving limbs as well as the specific activities performed, there are other issues with such solutions. Wearing one or multiple of such sensors on the body can be intrusive and

inconvenient for the user. Moreover, for long term monitoring they need to be recharged and maintained carefully by the users.

In order to overcome the limitations of both computer vision-based and wearable sensor-based systems, sensing through wireless signals has been considered for the recognition of human activities and gestures in general recently. In particular, usage of WiFi signals [11, 18, 29] has been studied extensively in the last years thanks to the already available WiFi devices and signals in most indoor environments. Most of these studies however consider a set of activities or gestures, depending on the application considered, and aim to recognize them through a machine learning based prediction model, without considering limb based decomposition. While in some earlier studies (e.g., CARM [33]), understanding the effects of different human body parts on the CSI has been slightly discussed, more related and detailed exploration is made only very recently through studies that look at the human pose estimation problem [21, 22, 36]. These studies however target estimation of joint locations and rotations and eventually the pose of the human mostly in static scenarios, which is different from our objective. They also leverage complicated hardware (e.g., L-shaped antenna) that can provide features like Angle of Arrival (AoA) thus are costly.

In terms of the machine learning solutions integrated in WiFi sensing studies, various different models and architectures have been considered including Dense Neural Networks (DNN) [10], Convolutional Neural Networks (CNN) [4], Long Short-Term Memory (LSTM) Networks [37] and Recurrent Neural Networks (RNN) [26] depending on the use case considered. Generative Adversarial Networks (GAN) [5, 6, 14, 32, 38] have also been considered to develop subject and environment independent generalized solutions. In this work we use GANs with a different purpose and aim to mitigate the temporal effect in the CSI data. That is, we consider data collected for the same activity at different times as different domains and minimize the effect of integrated temporal changes in them through the negative impact of domain discriminator. Furthermore, we integrate this GAN approach within our hierarchical based approach, making it different from previous studies.

3 PROPOSED SOLUTION

The proposed approach uses a hierarchical design in the prediction of limbs involved in the performed activity. Moreover, we use a GAN based neural network at each level. Next, we talk about the details of these two core components in our solution.

3.1 Hierarchical Prediction Approach

The proposed hierarchical approach breaks the task of recognition of a physical activity into subtasks and aims to recognize involved body limbs in that activity one by one. This is achieved through the usage of different prediction models at each level of the recognition hierarchy which are trained only with the data of the selected subset of activity classes.

We start with the first model, referred to as the *Level1* model, to determine which limb is the most prominent within this activity. Since there is no limb recognized yet at the beginning, this *Level1* model is the one that is pretrained with five individual limb movements only and aims to identify the mostly predicted one that is involved in the considered unknown (which can be single-limb or

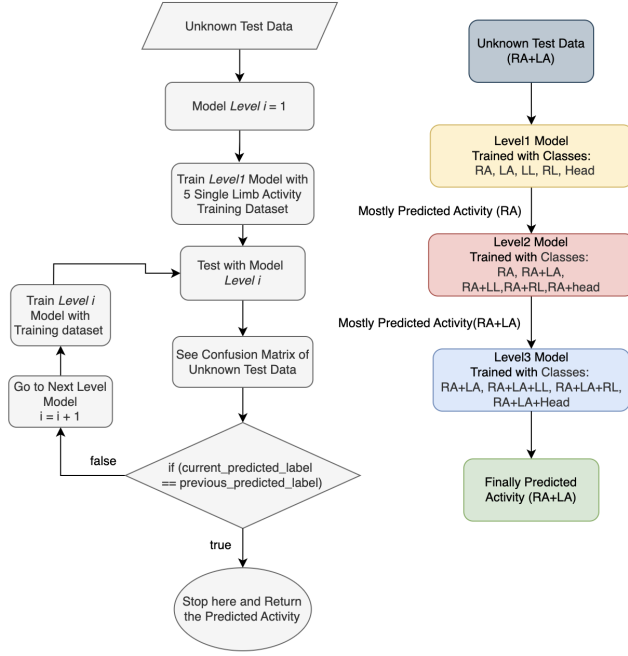


Figure 2: Steps of the proposed hierarchical prediction approach and an example run.

multi-limb) activity. Once this model predicts one of these five limbs (denoted as L_{pre}^1), we continue with the subsequent steps to identify the other limbs or stop the process of identifying new limbs. To this end, in the second level, we use a model that is trained with a set of classes that includes the class that is predicted in the previous level (i.e., L_{pre}^1) and all possible two limb combinations that include L_{pre}^1 . Once, the *Level2* model predicts the highest recognized class among them, we decide to continue or stop the recognition process depending on the prediction. That is, if *Level2* model predicts L_{pre}^1 with the highest prediction, we stop with the outcome from previous level; otherwise, we continue with the next level similarly.

Fig. 2 shows an example scenario for the unknown activity $RA+LA$ through this hierarchical prediction approach. After *Level1* model predicts RA with the highest ratio, we need a *Level2* model that is trained with classes that include RA class itself and the two limb classes that include RA (i.e., $RA+LA$, $RA+LL$, $RA+RL$ and $RA+Head$). Since the output of the *Level2* model is $RA+LA$, we continue with *Level3* with a model that is trained with class $RA+LA$ and all other three limb combinations that include $RA+LA$ (i.e., $RA+LA+LL$, $RA+LA+RL$, $RA+LA+Head$). *Level3* model predicts that $RA+LA$ is the highest predicted class, thus the process stops there. This depends on the insight that if no more limbs are included in an activity, the class representing the previous level prediction should be the highest.

Note that with this hierarchical approach, we consider smaller size models that are pretrained to recognize only a subset of limb combinations. With five limbs, there can be a total of $2^5 - 1 = 31$ different limb combinations moving in an activity potentially. Instead of a single model that is trained on all these combinations, the hierarchical approach overall depends on six 5-class classifiers (in

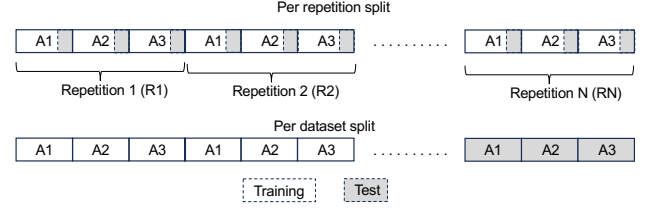


Figure 3: Two different ways of splitting dataset for training and testing.

Level1 and *Level2*), ten 4-class classifiers (in *Level3*), ten 3-class classifiers (in *Level4*) and five 2-class classifiers (in *Level5*) in total. This is to be ready for any unknown activity with any limb combination but indeed at each level only one model is used.

3.2 GAN Models to Mitigate Temporal Effects

Given this hierarchical classification approach, next, we need models at different levels for the subset of classes considered. To this end, we develop a GAN based architecture to mitigate any temporal effects in the data and obtain a generalized solution. In order to test the temporal effects in the data, we collected a dataset of activities repeated in a round robin fashion. This is achieved by collecting some data from each activity, and then starting another round of collection from each one again. Once the data is collected through multiple rounds, we considered two different splits of the data set into training and test portions as illustrated in Fig. 3. In the first way, we considered the last 30% of each repetition of each activity (i.e., gray areas) as test data, while in the second way we considered last 30% of the entire dataset as the testing part. Note that the latter is the proper way for temporal data, but our goal is to show how the temporal changes affect results. Our results show that with per repetition split, we can obtain much better prediction accuracy. This is because with per repetition split, the temporal difference between the training and test data is smaller thus the features learned by the model help recognize the features in test data. These results indicate that CSI dataset can have temporal effects and we need to handle that to obtain a robust prediction performance.

GAN based approach aims to address this issue. Note that while GANs have been considered by some previous work earlier [32, 38], the way we model it is different. We consider different repetitions of the activities collected as separate domains and design the domain discriminator to recognize such temporal differences when the same activity is performed. Thus, the negative impact of domain discriminator loss in GAN helps us recognize the activities properly even if they are performed at different times.

The main goal of this adversarial model is to extract temporal-independent but limb activity dependent features so that it can recognize any limb activity mitigating the environmental and temporal effects during the experiment.

To achieve this goal, the input data is initially transformed into low-dimensional representations (Z) by a feature extractor composed of a three-layer dense neural network (DNN). If X is the input dataset and P is considered as the set of all the parameters of DNN,

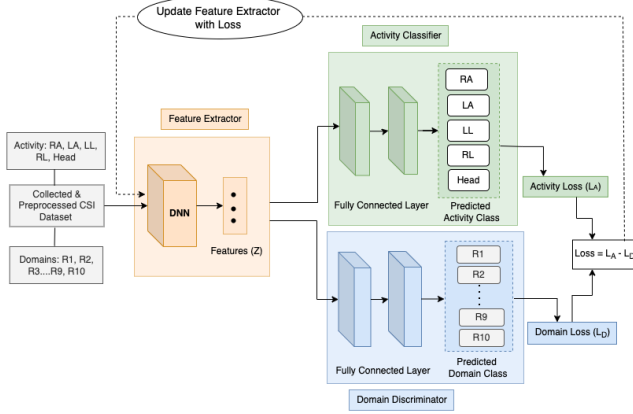


Figure 4: Proposed GAN network with repetitions representing different domains.

then learned features Z from the feature extractor can be written as $Z = DNN(X; P)$.

Utilizing these learned feature representations, the activity recognizer aims to maximize prediction accuracy by making predictions on all input data. To eliminate domain-specific features, a domain discriminator is employed to label each domain, identifying which activities are performed in which domain of the environment.

Ultimately the architecture of the model is built on three main blocks: (i) feature extractor, (ii) domain discriminator, and (iii) limb activity recognizer, as shown in Fig. 4. Our feature extractor model is a three-layer DNN which is designed to enhance feature learning and prevent overfitting. The first hidden layer comprises 128 neurons, utilizing the Rectified Linear Unit (ReLU) activation function to introduce non-linearity, followed by batch normalization to stabilize and accelerate the training process, and a dropout rate of 0.5 to mitigate overfitting by randomly deactivating half of the neurons during training. The second hidden layer consists of 64 neurons, also employing ReLU activation, batch normalization, and a dropout rate of 0.5, ensuring consistent regularization and normalization. The third hidden layer features 32 neurons with the same sequence of ReLU activation, batch normalization, and a dropout rate of 0.3.

Activity classifier and domain discriminator blocks are mainly built with fully connected layers for classifying activity and domain classes. Softmax is used as the activation function in both implementations.

In our study, the primary objective is to accurately recognize different activity classes formed by different limb movements. To achieve this, we need to optimize the feature extractor through backpropagation by minimizing the activity loss while simultaneously maximizing the domain loss. This approach ensures that the feature extractor can fool the domain discriminator and learn domain-independent features, enabling it to classify activities across various domains or different repetitions of the activities.

Table 1: Activities used in experiments together with the limbs involved in each activity.

	Limb Activity	RA	LA	LL	RL	Head
1	RA	✓				
2	LA		✓			
3	LL			✓		
4	RL				✓	
5	Head					✓
6	RA+LA	✓	✓			
7	RA+LL	✓		✓		
8	RA+RL	✓			✓	
9	LA+LL		✓	✓		
10	LA+RL		✓		✓	
11	LA+Head		✓			✓
12	RA+Head	✓				✓
13	LL+Head			✓		✓
14	RL+Head				✓	✓
15	RA+LA+Head	✓	✓			✓
16	RA+LA+LL	✓	✓	✓		
17	RA+LA+RL	✓	✓		✓	

4 EVALUATION

4.1 Experimental Set up and Data Collection

In order to test the performance of the proposed hierarchical approach, we collected WiFi CSI data for 17 different classes of movements that are given in Table 1. Note that we skipped some of the combinations (e.g., $LL+RL$ or $LA+RA+Head+LL$) due to the hardness of performing them. However, we will try to include more limb combinations in our future efforts.

We used our ESP32-CSI-Toolkit [7, 8] to collect CSI which uses two ESP32 WiFi-enabled microcontrollers for our transmitter and receiver, respectively. Note that these microcontrollers have very low cost (i.e., < \$10) allowing a more cheaper solution than wearable based tracking solutions, and without having the burden of intrusive nature of wearables. The ESP32 devices are set to transmit CSI at a packet rate of 100Hz.

Fig. 5 shows the scenario how ESP32 microcontrollers are setup during our data collection. Each activity is performed for 10 seconds (by moving the corresponding limbs included up and down at the same time), with a 10-second transition (i.e., no movement) period between activities. We repeated the 17 activities 10 times in a round robin fashion (as shown in Fig. 3), and these 10 repetitions were used as different domains in our deep learning model. Overall, the experiment took 56 minutes and 40 seconds.

4.2 CSI Pre-Processing

To prepare the dataset for our learning model, we apply several preprocessing steps after data collection. First, we convert the raw CSI data into CSI amplitude values for 64 different subcarriers of the channel by $A^{(i)} = \sqrt{(H_{im}^{(i)})^2 + (H_r^{(i)})^2}$, $H_r^{(i)}$ is the real and $H_{im}^{(i)}$ is the imaginary part of the CSI vector (H) for subcarrier i . We did not use the phase values in this study. After obtaining the amplitude values for all 64 subcarriers, we filter out the subcarriers whose

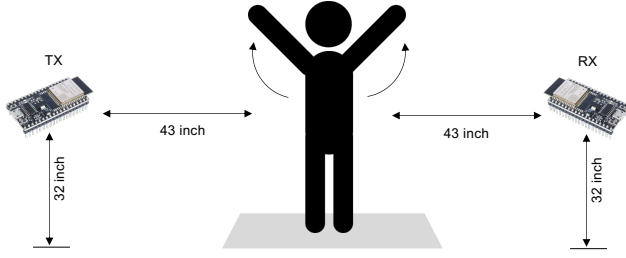


Figure 5: Experiment setup for data collection.

amplitude values remained constant over time. This process results in the exclusion of 12 subcarriers, leaving us with 52 subcarriers as the features for the input dataset.

Next, we apply window averaging to denoise and smooth the signal dataset. A sliding window function with a window size of 100 is used. After splitting the data into training and testing sets using dataset split as illustrated in Fig. 3, we then apply principal component analysis (PCA) to reduce the dimensionality of the dataset and extract the most relevant features. With these filtering and denoising methods, our dataset is prepared for model training.

4.3 Compared Prediction Models

We compare the following three different approaches:

All-class Classifiers: This refers to the straightforward approach with a model trained with data from all (i.e., 17) classes. We consider both a DNN and a GAN based model to show the benefit of GAN model within this case too. DNN model is structured similar to the feature extractor, activity classifier and domain discriminator architectures (e.g., ReLU activation, batch normalization, and a dropout layer) explained earlier for the GAN. For the loss function optimization, we used Adam optimizer with 0.02 as the learning rate and cross entropy loss as the loss function.

Multi-label Classifier: In this model, we consider labels of five limbs that are involved in each activity and train them with the corresponding labels. Table 1 shows these labels for each activity. We used the same DNN architecture here too. Due to multi-label design, each activity is encoded with binary codes of each limb. That is, for example, 'LA+RA' is encoded as 11000 and 'LA+LL' is encoded '01100', using the ordered labels of RA, LA, LL, RL and Head. Sigmoid activation function is applied at the fully connected layer. Binary cross entropy loss is also used as the loss function together with Adam optimizer.

GAN based Hierarchical Classifier: This refers to our proposed solution described in Section 3.

Each of these models are trained with 70% of the entire dataset collected and tested with the remaining 30% (i.e., dataset split). We also considered sliding windows for the CSI data before feeding them into each model. The window size is set to 100 (i.e., 1 sec of data).

RA	81%	28%	4%	0%	2%	12%	0%	4%	2%	1%	1%	0%	2%	0%	0%	0%	0%
LA	3%	50%	14%	0%	5%	7%	1%	3%	0%	1%	4%	2%	4%	0%	2%	1%	3%
LL	5%	0%	35%	8%	1%	2%	2%	3%	13%	3%	2%	2%	16%	7%	0%	1%	3%
RL	3%	3%	5%	27%	9%	3%	1%	6%	0%	8%	4%	2%	6%	9%	4%	3%	8%
Head	14%	4%	4%	0%	0%	56%	7%	0%	0%	0%	0%	0%	9%	0%	0%	4%	1%
RA+LA	100%	6%	8%	0%	1%	43%	6%	1%	3%	6%	8%	2%	2%	0%	2%	3%	0%
RA+LL	0%	0%	23%	2%	0%	0%	44%	10%	1%	0%	1%	0%	1%	1%	1%	9%	4%
RA+RL	5%	2%	9%	3%	0%	1%	2%	27%	12%	8%	3%	2%	13%	1%	0%	4%	9%
LA+LL	2%	0%	16%	1%	1%	0%	11%	4%	18%	4%	2%	1%	13%	6%	0%	1%	1%
LA+RL	4%	0%	4%	4%	0%	7%	0%	8%	0%	17%	6%	6%	2%	19%	0%	3%	0%
LA+Head	10%	0%	3%	0%	2%	2%	0%	1%	0%	11%	19%	31%	1%	9%	6%	3%	1%
RA+Head	3%	0%	9%	0%	1%	1%	0%	0%	2%	2%	8%	57%	8%	6%	6%	0%	0%
LL+Head	2%	1%	11%	8%	0%	2%	3%	3%	1%	6%	2%	0%	27%	28%	2%	0%	5%
RL+Head	1%	0%	0%	7%	0%	3%	0%	1%	0%	9%	1%	3%	4%	63%	4%	0%	0%
RA+LA+Head	11%	5%	0%	3%	5%	3%	0%	4%	1%	4%	4%	35%	1%	3%	34%	5%	1%
RA+LA+LL	0%	2%	5%	3%	0%	0%	16%	7%	3%	4%	2%	0%	16%	5%	0%	30%	8%
RA+LA+RL	15%	0%	1%	19%	0%	0%	0%	11%	0%	6%	0%	0%	1%	8%	3%	0%	17%
Head	14%	4%	4%	0%	0%	56%	7%	0%	0%	0%	0%	0%	9%	0%	0%	4%	1%
RA+LA	100%	6%	8%	0%	1%	43%	6%	1%	3%	6%	8%	2%	2%	0%	2%	3%	0%
RA+LL	0%	0%	23%	2%	0%	0%	44%	10%	1%	0%	1%	0%	1%	1%	1%	9%	4%
RA+RL	5%	2%	9%	3%	0%	1%	2%	27%	12%	8%	3%	2%	13%	1%	0%	4%	9%
LA+LL	2%	0%	16%	1%	1%	0%	11%	4%	18%	4%	2%	1%	13%	6%	0%	1%	1%
LA+RL	4%	0%	4%	4%	0%	7%	0%	8%	0%	17%	6%	6%	2%	19%	0%	3%	0%
LA+Head	10%	0%	3%	0%	2%	2%	0%	1%	0%	11%	19%	31%	1%	9%	6%	3%	1%
RA+Head	3%	0%	9%	0%	1%	1%	0%	0%	2%	2%	8%	57%	8%	6%	6%	0%	0%
LL+Head	2%	1%	11%	8%	0%	2%	3%	3%	1%	6%	2%	0%	27%	28%	2%	0%	5%
RL+Head	1%	0%	0%	7%	0%	3%	0%	1%	0%	9%	1%	3%	4%	63%	4%	0%	0%
RA+LA+Head	11%	5%	0%	3%	5%	3%	0%	4%	1%	4%	4%	35%	1%	3%	34%	5%	1%
RA+LA+LL	0%	2%	5%	3%	0%	0%	16%	7%	3%	4%	2%	0%	16%	5%	0%	30%	8%
RA+LA+RL	15%	0%	1%	19%	0%	0%	0%	11%	0%	6%	0%	0%	1%	8%	3%	0%	17%

Figure 6: Confusion Matrix of 17-class DNN classifier.

4.4 Performance Metrics

We use two main metrics, namely, prediction accuracy and Hamming loss. Accuracy is defined as the ratio of the number of correctly predicted instances to the total number of the instances in the test data:

$$\text{Accuracy} = \frac{\text{TP} + \text{TN}}{\text{TP} + \text{TN} + \text{FP} + \text{FN}}$$

where TP is true positives, TN is true negatives, FP is false positives and FN is false negatives. Note that since our activities include multiple labels, for a prediction to be TP, all the labels should be correctly predicted, thus an exact matching is required. Thus, to quantify the difference between the set of the true labels and the set of the predicted labels, we also use Hamming loss for a more detailed prediction analysis. Hamming loss can be calculated by applying the XOR function for each instance and then adding them together to find the overall measurement [12]:

$$\text{Hamming loss} = \frac{1}{m} \sum_{i=1}^m \frac{1}{q} \Delta(T_i, P_i)$$

where m is the number of samples, T_i and P_i are the list of true and predicted labels of instance i , respectively, q is the number of classes used in the prediction model, and $\Delta(\cdot)$ is the XOR function that gives the number of classes that are wrongly predicted for each instance.

4.5 Performance Results

First of all, we look at the results with all class classifiers. While considering a single model trained with all classes can be a straightforward solution, our results show that we can only get 33 and 42% accuracy with a DNN and GAN-based 17-class classifiers, respectively. Looking at Fig. 6 which shows the confusion matrix of the 17-class DNN classifier results, we see that the diagonal has the highest prediction values. However, we notice that a multi-limb activity can be confused with the single limb activities it contains. For example, *RA+LA* is confused with single limb activity *RA*; *RA+LL* is confused with *LL*. Similarly, we see confusions between the multi-limb activities which have limb(s) in common (e.g., *LL+Head* with *RL+Head*).

Table 2: Multi Label Classifier Results

	Unknown Limb Activity	Accuracy (%) (exact match)	Hamming Loss
1	RA	47.44	0.1812
2	LA	56.94	0.1334
3	LL	53.22	0.1365
4	RL	43.26	0.1575
5	Head	50.28	0.1674
6	RA+LA	61.88	0.1058
7	RA+LL	61.91	0.0933
8	RA+RL	40.85	0.1785
9	LA+LL	56.33	0.1267
10	LA+RL	41.76	0.1934
11	LA+Head	41.53	0.1817
12	RA+Head	67.70	0.0820
13	LL+Head	33.99	0.2178
14	RL+Head	59.25	0.1149
15	RA+LA+Head	51.58	0.1278
16	RA+LA+LL	53.58	0.1491
17	RA+LA+RL	52.85	0.1384

Table 3: Prediction results at each level by the proposed hierarchical GAN based hierarchical approach.

	Unknown Limb Activity	Level 1	Level 2	Level 3
		Highest predicted class		
1	RA	RA	RA+LA	N/A
2	LA	LA	LA	
3	LL	LL	LL	
4	RL	RL	RL	
5	Head	Head	Head	
6	RA+LA	LA	RA+LA	RA+LA
7	RA+LL	LL	RA+LL	RA+LL
8	RA+RL	RL	RL	
9	LA+LL	LL	LA+LL	LA+LL
10	LA+RL	RL	RA+RL	
11	LA+Head	LA	LA+Head	LA+Head
12	RA+Head	RA	RA+Head	RA+Head
13	LL+Head	LL	LL+Head	No data
14	RL+Head	RL	RL+Head	No data
15	RA+LA+Head	RA	RA+LA	RA+LA+Head
16	RA+LA+LL	LL	RA+LL	RA+LA+LL
17	RA+LA+RL	RL	RL	

The results for multi-label classifier model is given in Table 2. We see that the accuracy for classes ranges between 33.99% and 67.70%, with an average of 51.43%. Hamming loss ranges between 0.082 and 0.2178, with an average of 0.1464. Even though the results are better than all-class classifier results, it may not be sufficient to be used in practice.

Finally, we look at the results of the proposed hierarchical GAN based approach. The results in Table 3 shows the highest predicted class for each unknown class at each level of recognition process.

Table 4: Performance Comparison of Different Approaches

Prediction Model	Accuracy (%) (exact match)	Hamming Loss (%)
All-class classifier (DNN)	33.39	0.1764
All-class classifier (GAN)	42.87	0.1512
Multi-label Classifier	51.43	0.1464
GAN based Hierarchical Classifier	76.47	0.0705

We see that our *Level1* GAN models always predict a correct limb included in the unknown activity considered. In *Level2*, we see failures in four cases, that are highlighted and strike through. For example, for *RA*, *Level2* model should predict *RA* as the highest predicted class but it predicts *RA+LA* as the highest. Digging further, we find that in all these four failing cases, our GAN models actually predict the right class as the second highest predicted class. That is why when we look at the Hamming loss obtained from these predictions, we see 0.0705, which shows the true predictions (i.e., exact match) are indeed slightly missed.

Note that in some scenarios, we could not get results for each level towards the stopping criteria defined. For example, for *LL+Head*, we could not test if the proposed method would select *LL+Head* in *Level3* due to the lack of data. Similarly, for *RA+LA+Head*, we predict correctly in all three levels but we need to test if the proposed method would select *RA+LA+Head* in *Level4* too to stop the process. However, this is skipped as collecting four limb movements was challenging.

Overall, as Table 4 shows, the proposed GAN-based hierarchical recognition approach achieves the highest accuracy and the lowest Hamming loss among all models compared. In the future, we will consider more combinations of limbs and evaluate the performance in the missing possible scenarios.

5 CONCLUSION

In this work, we studied the use of CSI data from WiFi signals to recognize the limbs involved in a physical activity. We proposed a hierarchical approach that aims to recognize the involved limbs in the activity one by one. We used GAN based models at each level of recognition steps and utilized a stopping method that does not proceed to further levels if the predicted class is still from previous level. The performance evaluation shows that the proposed approach shows a higher prediction accuracy and a low Hamming loss, compared to other solutions.

While there is room to improve these results, we would like to note that these results are obtained with only one TX-RX link in the environment. In our future efforts, we will consider more TX-RX pairs distributed in the area. We will also consider different moving speeds for each limb and try to recognize these speeds for the identified models. Finally, we will collect data from more volunteers and evaluate the robustness of our approach.

REFERENCES

- [1] Claire L Bentley, Lauren Powell, Stephen Potter, Jack Parker, Gail A Mountain, Yvonne Kiera Bartlett, Jochen Farwer, Cath O'Connor, Jennifer Burns, Rachel L Cresswell, et al. 2020. The use of a smartphone app and an activity tracker to promote physical activity in the management of chronic obstructive pulmonary disease: randomized controlled feasibility study. *JMIR mHealth and uHealth* 8, 6 (2020), e16203.
- [2] Zhe Cao, Tomas Simon, Shih-En Wei, and Yaser Sheikh. 2017. Realtime multi-person 2d pose estimation using part affinity fields. In *Proceedings of the IEEE conference on computer vision and pattern recognition*. 7291–7299.
- [3] Chen Chen, Gang Zhou, and Youfang Lin. 2023. Cross-domain wifi sensing with channel state information: A survey. *Comput. Surveys* 55, 11 (2023), 1–37.
- [4] Hadi El Zein, Farah Mourad-Chehade, and Hassan Amoud. 2024. CSI-based Human Activity Recognition via Lightweight CNN Model and Data Augmentation. *IEEE Sensors Journal* (2024).
- [5] Yaroslav Ganin and Victor Lempitsky. 2015. Unsupervised domain adaptation by backpropagation. In *International conference on machine learning*. PMLR, 1180–1189.
- [6] Ian J. Goodfellow, Jean Pouget-Abadie, Mehdi Mirza, Bing Xu, David Warde-Farley, Sherjil Ozair, Aaron Courville, and Yoshua Bengio. 2014. Generative Adversarial Networks. (2014). arXiv:1406.2661 [stat.ML] <https://arxiv.org/abs/1406.2661>
- [7] Steven M. Hernandez. 2023. ESP32 CSI Tool. <https://stevenmhernandez.github.io/ESP32-CSI-Tool/>
- [8] Steven M Hernandez and Eyuphan Bulut. 2020. Lightweight and Standalone IoT based WiFi Sensing for Active Repositioning and Mobility. In *21st International Symposium on "A World of Wireless, Mobile and Multimedia Networks" (WoWMoM)*. Cork, Ireland.
- [9] Steven M Hernandez and Eyuphan Bulut. 2021. WiFederated: Scalable WiFi sensing using edge-based federated learning. *IEEE Internet of Things Journal* 9, 14 (2021), 12628–12640.
- [10] Steven M Hernandez and Eyuphan Bulut. 2022. Wifi sensing on the edge: Signal processing techniques and challenges for real-world systems. *IEEE Communications Surveys & Tutorials* 25, 1 (2022), 46–76.
- [11] Steven M Hernandez and Eyuphan Bulut. 2020. Performing WiFi Sensing with Off-the-shelf Smartphones. In *IEEE International Conference on Pervasive Computing and Communications Workshops (PerCom Workshops)*. 1–3.
- [12] Mohammadreza Heydari, Thomas E Doyle, and Reza Samavi. 2022. MLCM: Multi-label confusion matrix. *IEEE Access* 10 (2022), 19083–19095.
- [13] Shang-Rung Hwang, Sheng-Wei Hwang, Jin-Cherng Chen, and Juen-Haur Hwang. 2019. Association of periodic limb movements during sleep and Parkinson disease: A retrospective clinical study. *Medicine* 98, 51 (2019), e18444.
- [14] Wenjun Jiang, Chenglin Miao, Fenglong Ma, Shuochao Yao, Yaqing Wang, Ye Yuan, Hongfei Xue, Chen Song, Xin Ma, Dimitrios Koutsonikolas, et al. 2018. Towards environment independent device free human activity recognition. In *Proceedings of the 24th annual international conference on mobile computing and networking*. 289–304.
- [15] Charlotte Kerner, Adam Burrows, and Bronagh McGrane. 2019. Health wearables in adolescents: implications for body satisfaction, motivation and physical activity. *International Journal of Health Promotion and Education* 57, 4 (2019), 191–202.
- [16] Jungyoon Kim, Songhee Cheon, and Jihye Lim. 2022. IoT-based unobtrusive physical activity monitoring system for predicting dementia. *Ieee Access* 10 (2022), 26078–26089.
- [17] Yang Liu, Zhenjiang Li, Zhidan Liu, and Kaishun Wu. 2019. Real-time arm skeleton tracking and gesture inference tolerant to missing wearable sensors. In *Proceedings of the 17th Annual International Conference on Mobile Systems, Applications, and Services*. 287–299.
- [18] Yongsan Ma, Gang Zhou, and Shuangquan Wang. 2019. WiFi Sensing with Channel State Information: A Survey. *ACM Comput. Surv.* 52, 3 (2019), 46:1–46:36. <https://doi.org/10.1145/3310194>
- [19] George Papandreou, Tyler Zhu, Nori Kanazawa, Alexander Toshev, Jonathan Tompson, Chris Bregler, and Kevin Murphy. 2017. Towards accurate multi-person pose estimation in the wild. In *Proceedings of the IEEE conference on computer vision and pattern recognition*. 4903–4911.
- [20] Dario Pavlo, Christoph Feichtenhofer, David Grangier, and Michael Auli. 2019. 3d human pose estimation in video with temporal convolutions and semi-supervised training. In *Proceedings of the IEEE/CVF conference on computer vision and pattern recognition*. 7753–7762.
- [21] Yili Ren, Zi Wang, Sheng Tan, Yingying Chen, and Jie Yang. 2021. Winect: 3d human pose tracking for free-form activity using commodity wifi. *Proceedings of the ACM on Interactive, Mobile, Wearable and Ubiquitous Technologies* 5, 4 (2021), 1–29.
- [22] Yili Ren, Zi Wang, Yichao Wang, Sheng Tan, Yingying Chen, and Jie Yang. 2022. GoPose: 3D human pose estimation using WiFi. *Proceedings of the ACM on Interactive, Mobile, Wearable and Ubiquitous Technologies* 6, 2 (2022), 1–25.
- [23] Alexander Seifert, Anna Schlomann, Christian Rietz, and Hans Rudolf Schelling. 2017. The use of mobile devices for physical activity tracking in older adults' everyday life. *Digital health* 3 (2017), 2055207617740088.
- [24] Sheng Shen, Mahanth Gowda, and Romit Roy Choudhury. 2018. Closing the gaps in inertial motion tracking. In *Proceedings of the 24th Annual International Conference on Mobile Computing and Networking*. 429–444.
- [25] Sheng Shen, He Wang, and Romit Roy Choudhury. 2016. I am a smartwatch and i can track my user's arm. In *Proceedings of the 14th annual international conference on Mobile systems, applications, and services*. 85–96.
- [26] Zhenguo Shi, Qingqing Cheng, J Andrew Zhang, and Richard Yi Da Xu. 2022. Environment-robust WiFi-based human activity recognition using enhanced CSI and deep learning. *IEEE Internet of Things Journal* 9, 24 (2022), 24643–24654.
- [27] Patrick Slade, Mykel J Kochenderfer, Scott L Delp, and Steven H Collins. 2021. Sensing leg movement enhances wearable monitoring of energy expenditure. *Nature Communications* 12, 1 (2021), 4312.
- [28] Tessa Strain, Katrien Wijndaele, Paddy C Dempsey, Stephen J Sharp, Matthew Pearce, Justin Jeon, Tim Lindsay, Nick Wareham, and Søren Brage. 2020. Wearable-device-measured physical activity and future health risk. *Nature medicine* 26, 9 (2020), 1385–1391.
- [29] Sheng Tan, Yili Ren, Jie Yang, and Yingying Chen. 2022. Commodity WiFi sensing in ten years: Status, challenges, and opportunities. *IEEE Internet of Things Journal* 9, 18 (2022), 17832–17843.
- [30] Md Touhiduzzaman, Steven M Hernandez, Peter E Pidcoe, and Eyuphan Bulut. 2024. Wi-PT-Hand: Wireless Sensing based Low-cost Physical Rehabilitation Tracking for Hand Movements. *ACM Transactions on Computing for Healthcare* (2024).
- [31] Erdenebayar Urtnasan, Jong-Uk Park, Jung-Hun Lee, Sang-Baek Koh, and Kyoung-Joung Lee. 2022. Deep learning for automatic detection of periodic limb movement disorder based on electrocardiogram signals. *Diagnostics* 12, 9 (2022), 2149.
- [32] Jiwei Wang, Yiqiang Chen, Yang Gu, Yunlong Xiao, and Haonan Pan. 2018. SensoryGANs: An Effective Generative Adversarial Framework for Sensor-based Human Activity Recognition. In *2018 International Joint Conference on Neural Networks (IJCNN)*. 1–8. <https://doi.org/10.1109/IJCNN.2018.8489106>
- [33] Wei Wang, Alex X Liu, Muhammad Shahzad, Kang Ling, and Sanglu Lu. 2015. Understanding and modeling of wifi signal based human activity recognition. In *Proceedings of the 21st annual international conference on mobile computing and networking*. 65–76.
- [34] Tom White, Kate Westgate, Stefanie Hollidge, Michelle Venables, Patrick Olivier, Nick Wareham, and Soren Brage. 2019. Estimating energy expenditure from wrist and thigh accelerometry in free-living adults: a doubly labelled water study. *International journal of obesity* 43, 11 (2019), 2333–2342.
- [35] Yoram Wurmser. 2023. The smart wearables market is growing older. <https://www.emarketer.com/content/smart-wearables-market-growing-older>
- [36] Mingming Xu, Zhengxin Guo, Linqing Gui, Biyun Sheng, and Fu Xiao. 2023. WiSPE: A COTS Wi-Fi-Based 2-D Static Human Pose Estimation. *IEEE Systems Journal* 17, 3 (2023), 3560–3571.
- [37] Jin Zhang, Fuxiang Wu, Bo Wei, Qieshi Zhang, Hui Huang, Syed W Shah, and Jun Cheng. 2020. Data augmentation and dense-LSTM for human activity recognition using WiFi signal. *IEEE Internet of Things Journal* 8, 6 (2020), 4628–4641.
- [38] Siwang Zhou, Wei Zhang, Dan Peng, Yonghe Liu, Xingwei Liao, and Hongbo Jiang. 2019. Adversarial WiFi sensing for privacy preservation of human behaviors. *IEEE Communications Letters* 24, 2 (2019), 259–263.